

Excitation-power-dependent upconversion luminescence competition in single β -NaYbF₄:Er microcrystal pumped at 808 nm

Maohui Yuan

National University of Defense Technology College of Advanced Interdisciplinary Studies

Zining Yang

National University of Defense Technology College of Advanced Interdisciplinary Studies

Xu Yang

National University of Defense Technology College of Advanced Interdisciplinary Studies

Linxuan Wang

National University of Defense Technology College of Advanced Interdisciplinary Studies

Rui Wang

National University of Defense Technology College of Advanced Interdisciplinary Studies

Sheng Lan

South China Normal University Guangzhou Higher Education Mega Center

Kai Han

National University of Defense Technology College of Advanced Interdisciplinary Studies

Hongyan Wang (✉ wanghongyan@nudt.edu.cn)

National University of Defense Technology <https://orcid.org/0000-0001-5390-5813>

Xiaojun Xu

National University of Defense Technology College of Advanced Interdisciplinary Studies

Nano Express

Keywords: Single NaYbF₄:Er microcrystals, Upconversion luminescence, 808 nm excitation, Excitation-power-dependent, Multicolor

Posted Date: September 15th, 2021

DOI: <https://doi.org/10.21203/rs.3.rs-903372/v1>

License:   This work is licensed under a Creative Commons Attribution 4.0 International License.

[Read Full License](#)

Excitation-power-dependent upconversion luminescence competition in single β -NaYbF₄:Er microcrystal pumped at 808 nm

Maohui Yuan,^{1,4,6} Zining Yang,^{1,2,3,6} Xu Yang,^{1,2,3} Linxuan Wang,^{1,2,3} Rui Wang,^{1,2,3,6} Sheng Lan,⁵ Kai Han,^{1,2,3,*} Hongyan Wang,^{1,2,3,*} and Xiaojun Xu^{1,2,3}

¹College of Advanced Interdisciplinary Studies, National University of Defense Technology, Changsha, 410073, China

²State Key Laboratory of Pulsed Power Laser Technology, National University of Defense Technology, Changsha, 410073, China

³Hunan Provincial Key Laboratory of High Energy Laser Technology, National University of Defense Technology, Changsha, 410073, China

⁴Department of physics and chemistry, PLA Army Academy of Special Operations, Guangzhou 510507, China

⁵Guangdong Provincial Key Laboratory of Nanophotonic Functional Materials and Devices, School of Information and Optoelectronic Science and Engineering, South China Normal University, Guangzhou, 510006, China

⁶Maohui Yuan and Zining Yang contributed equally to this work.

*Corresponding author: hankai0071@nudt.edu.cn and wanghongyan@nudt.edu.cn

Abstract: Controlling the upconversion luminescence (UCL) intensity ratio, especially pumped at 808 nm, is of fundamental importance in biological applications due to the water molecules exhibiting low absorption at this excitation wavelength. In this work, a series of β -NaYbF₄:Er microrods were synthesized by a simple one-pot hydrothermal method and their intense green (545 nm) and red (650 nm) UCL were experimentally investigated based on single particle level under the excitation of 808 nm continuous-wave (CW) laser. Interestingly, the competition between the green and red UCL can be observed in highly Yb³⁺-doped microcrystals as the excitation intensity gradually increases, which leads to the UCL color changes from green to orange. However, the microcrystals doped with low Yb³⁺ concentration keep green color which is independent on the excitation power. Further investigations demonstrate that the cross-relaxation (CR) processes between Yb³⁺ and Er³⁺ ions result in the UCL competition.

Keywords: Single NaYbF₄:Er microcrystals, Upconversion luminescence, 808 nm excitation, Excitation-power-dependent, Multicolor

1. Introduction

Rare-earth-ion doped UC nanomaterials have drawn a great attention recently due to their promising applications in biological issues [1], super-resolutions imaging [2], multicolor display [3], thermometer sensor [4], laser refrigeration [5-6], and laser materials [7-8]. These UC nanomaterials can efficiently convert the near infrared light into visible emissions according to the anti-Stokes process. Generally, the achieving of UCL relies on the sensitizer-activator pair. To obtain the efficient UCL, the sensitizer-activator pair of lanthanides should incorporate in

appropriate host lattices [9]. To date, the NaYF₄ has been considered to the most efficient host for generating UCL owing to its low phonon energy (~350 cm⁻¹) [10]. In general, the typical Yb³⁺ ions act as the sensitizer absorbing the excitation energy and the activator of Er³⁺ (Tm³⁺ or Ho³⁺) is responsible for emitting the UCL [11-13].

It is well-known that the Yb³⁺ ions have large absorption cross-section at 980 nm, which can be efficiently excited by the high-performance and commercial laser diode [14]. However, owing to the large absorption coefficient of water molecules at 980 nm, the Yb³⁺-sensitized UC nanoparticles would face severe overheating problems, which limits its further application in biological tissues and aqueous environment by decreasing the depth of penetration [15]. To overcome the overheating effects, the conventional approach is to dope Nd³⁺ ions as sensitizer which can shift the excitation wavelength from 980 to 808 nm [16-17]. Nonetheless, the dopant of Nd³⁺ usually yields small nanoparticles and hardly grows to microcrystals due to the larger Nd³⁺ ($r = 1.249 \text{ \AA}$) substitution of the relatively smaller Y³⁺ ($r = 1.159 \text{ \AA}$) in NaYF₄ lattice [10]. Importantly, compared with the nano-scale UC particles, micro-scale UC particles facilitate more advantages for applications in micro-optoelectronic devices, volumetric color display, and microlasers based on their high crystallinity and luminescent efficiency [18-22]. However, the most present researches are mainly conducted in aqueous solutions, organic solvents or as-prepared solid powders. This may lead to severe overheating problems and the UCL will be influenced by the adjacent particles. Therefore, exploring the UCL and tunable color in single microparticle level, especially pumped at 808 nm wavelength, will effectively avoid the effects of external environment and broaden its further applications in micro-optoelectronic devices and aqueous environment.

In this study, we firstly report the effect of excitation-power-dependent UCL competition in single Yb³⁺-sensitized NaYbF₄:Er microcrystal pumped at 808 nm. The properties of the UCL competition are characterized by the single microcrystal level. The competition between green and red UCL is clearly observed in highly Yb³⁺-doped microcrystals with varying the excitation intensity, and the UCL color was tuned from green to orange. On the contrary, there is no UCL competitions observed in lowly Yb³⁺-doped microcrystal and the UCL color always maintains green which is independent on the excitation power. The mechanism of the UCL competition is also demonstrated in detail.

2. Experimental Sections

2.1 Chemicals

The chemicals of rare-earth (RE) nitrates (Y(NO₃)₃, Yb(NO₃)₃ and Er(NO₃)₃, 99.9%), nitric acid (HNO₃, AR), Ethylenediamine tetraaceticacid disodium salt dihydrate (EDTA-2Na, AR), sodium hydroxide (NaOH, AR) and ammonium fluoride (NH₄F, AR) were purchased from Aladdin (China). All the chemicals were directly used as received without further purification.

2.2 Synthesis of β -NaYbF₄ microcrystals

The β -NaYbF₄:Er microcrystals were synthesized by the similar hydrothermal method procedure according to our previous study [23]. In a typical procedure, for instance, synthesis of the β -NaYbF₄:2%Er (mol%) microcrystals: firstly, the Yb(NO₃)₃ and Er(NO₃)₃ powders were dissolved in deionized water yielding a clear solution of Ln(NO₃)₃ (0.2 M); then the EDTA-2Na (1 mmol) and NaOH (5 mmol) were mixed

with 12.5 mL deionized water under continuously stirring in a beaker; following, 5 mL of $\text{Ln}(\text{NO}_3)_3$ (0.2 M) aqueous solutions (the total Ln^{3+} is 1 mmol), 8 mL of NH_4F (2.0 M) aqueous solutions and 7 mL of dilute hydrochloric acid (1 M) were added into the beaker; finally, the above mixtures were stirred for 1.5 hour and transferred into a 50 mL Teflon-lined autoclave and heated at 200°C for 40 hours. The as-prepared white precipitates were collected by centrifugation, washed with DI water and ethanol for several times, and dried in air at 40°C for 8 hours. The microcrystals doped with different concentrations of Yb^{3+} or Er^{3+} can be similarly synthesized by varying the volume of $\text{Ln}(\text{NO}_3)_3$ aqueous solutions.

2.3 Structural Characterization

The morphology and size of the $\beta\text{-NaYbF}_4\text{:Er}$ microcrystals were characterized by scanning electron microscope (SEM) (S4800, Hitachi). X-ray diffraction (XRD) patterns of the microcrystals were measured using powder X-ray diffractometer (Rigaku).

2.4 Upconversion luminescence measurements

In the photoluminescence experiments, the 808 nm CW laser was integrated with an inverted microscope (Observer A1, Zeiss) and irradiated on the microcrystals with a $100\times$ objective lens ($\text{NA}=1.4$). The diameter of the excitation spot was estimated to be $\sim 2.0\ \mu\text{m}$. The UCL generated from the microcrystals was collected by the same objective lens and then transmitted to a spectrometer (SR-500I-B1, Andor) coupled with a charge-coupled device (DU970N, Andor) for optical signal analysis. The UCL colors of the microcrystals were photographed using a high sensitivity of camera (DS-Ri2, Nikon).

3. Results and discussion

Fig. 1a-c shows the SEM images of the as-prepared $\beta\text{-NaYbF}_4\text{:Er}$ microcrystals doped with different Yb^{3+} concentrations. The results indicate that the microcrystals exhibit the hexagonal prism morphology and uniform size distribution (with the lengths of $\sim 15\ \mu\text{m}$ and diameters of $\sim 6\ \mu\text{m}$). Notably, adjusting the doping Yb^{3+} concentrations slightly varies the size of microcrystals. Fig. 1d gives the elements mapping of single $\text{NaYF}_4\text{:60%Yb,2%Er}$ microcrystal, which clearly demonstrates that the Y^{3+} , Yb^{3+} and Er^{3+} ions are homogeneously incorporated in the NaYF_4 host lattices. Fig. 1e displays the XRD patterns of the $\beta\text{-NaYF}_4\text{:x%Yb,2%Er}$ microcrystals with different Yb^{3+} concentrations. It reveals

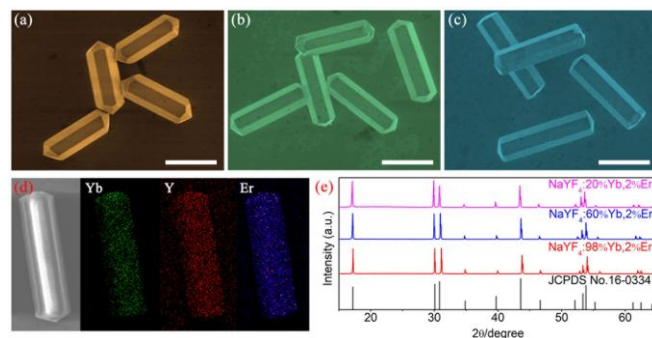


Fig. 1. SEM images of the (a) $\beta\text{-NaYF}_4\text{:98%Yb,2%Er}$, (b) $\beta\text{-NaYF}_4\text{:60%Yb,2%Er}$, (c) $\beta\text{-NaYF}_4\text{:20%Yb,2%Er}$ microcrystals. The scale bar is $10\ \mu\text{m}$. (d) The elements mapping of the $\beta\text{-NaYF}_4\text{:60%Yb,2%Er}$ microcrystals. (e) XRD patterns of the $\beta\text{-NaYF}_4\text{:x%Yb,2%Er}$ microcrystals.

that all the diffraction peaks are well in accordance with the standard hexagonal phases of NaYF₄ host (JCPDS No. 16-0334). The SEM images and XRD patterns confirm that the NaYF₄ microcrystals are successfully synthesized and highly crystalline.

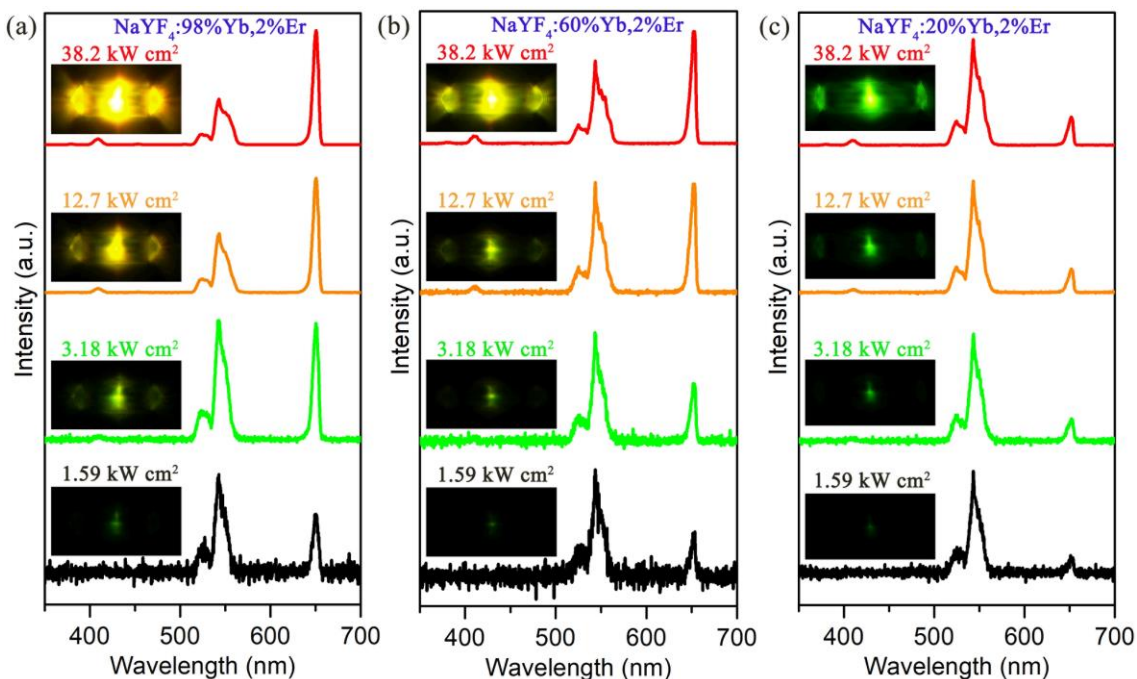


Fig. 2. The UCL spectra of single (a) β -NaYF₄:98%Yb,2%Er, (b) β -NaYF₄:60%Yb,2%Er, (c) β -NaYF₄:20%Yb,2%Er microcrystal under the excitation of 808 nm CW laser with different excitation density. The insert UCL photographs are corresponding to the relevant spectrum, respectively.

Fig. 2 shows the UCL spectra of single β -NaYF₄:x%Yb,2%Er microcrystal under the excitation of 808 nm CW laser with different excitation density. The corresponding UCL photographs are also provided in the inserts of relevant spectrum, respectively. Fig. 2a gives the spectra of the highly Yb³⁺-doped single NaYbF₄:2%Er microcrystal. The typical green (525 and 545 nm) and red (650 nm) UCL can be clearly observed, which are ascribed to the transitions of (²H_{11/2}/⁴S_{3/2})→⁴I_{15/2} and ⁴F_{9/2}→⁴I_{15/2} from Er³⁺, respectively. Under the excitation density of 1.59 kW cm⁻², the relatively weak green and red UCL emerge in the spectrum. The intensity of the green (545 nm) UC emission is larger than the red (650 nm) one, leading to the single hexagonal microcrystal exhibiting green color. As the excitation intensity slightly increases to 3.18 kW cm⁻², the red UCL increases more fast than the green UCL and their intensities are almost equal. This results in the UCL color changing to dark yellow. Notably, it can clearly observe that the UC emissions are transparent to the hexagonal microcrystal and transport from middle of the microrod to the two side ports. This phenomenon has also been demonstrated in previous literatures [21, 24]. When further rises the excitation intensity up to 12.7 kW cm⁻², the red UCL enhances rapidly and exceeds the green UC emission, which causes the luminescence color tuning to yellow. Moreover, a new blue UCL centered at 410 nm appears, which is originated from the transition of ²H_{9/2}→⁴I_{15/2} from Er³⁺. As the excitation intensity continues to increase to 38.2 kW cm⁻², the red UCL increases remarkably and further surpasses the green UC emission leading to the UCL color turning into orange. The results demonstrate that the green and red UCL compete to each other as varies the excitation power. It is the first time that the UCL competition is observed in Er³⁺ ions for the highly Yb³⁺-doped micromaterials pumped at 808 nm.

To explore the influence of the Yb^{3+} concentration on the UCL competition, we further investigate the UCL properties of the single $\text{NaYF}_4:x\%\text{Yb},2\%\text{Er}$ microcrystal doped with different Yb^{3+} concentrations. Fig. 2b displays the UCL spectra of the single $\text{NaYF}_4:60\%\text{Yb},2\%\text{Er}$ microcrystal. The same phenomenon to the microcrystal doped with 98% Yb^{3+} can be observed (Fig. 1a). Differently, the red UCL exceeds the green UCL at a relatively high excitation intensity which is higher than that of the $\text{NaYF}_4:98\%\text{Yb},2\%\text{Er}$ microcrystal. Moreover, the UCL color of the single $\text{NaYF}_4:60\%\text{Yb},2\%\text{Er}$ microcrystal changes from green to yellow as the excitation intensity increases. However, as shown in Fig. 2c, when the doping Yb^{3+} ions further decrease to 20%, the green and red UCL keep the similar growth trend as the excitation intensity gradually reinforces. This leads to the UCL color maintaining green and no UCL competition occurs in the single microcrystal. Thus, the results verify that the highly Yb^{3+} -doped microcrystals can efficiently generate the green and red UCL competition, causing the UCL color tuning from green to orange with increasing the excitation intensity. In contrast, for lowly Yb^{3+} -doped microcrystals, the green UCL is always larger than the red one and the UCL color is green regardless of the variation of excitation intensity.

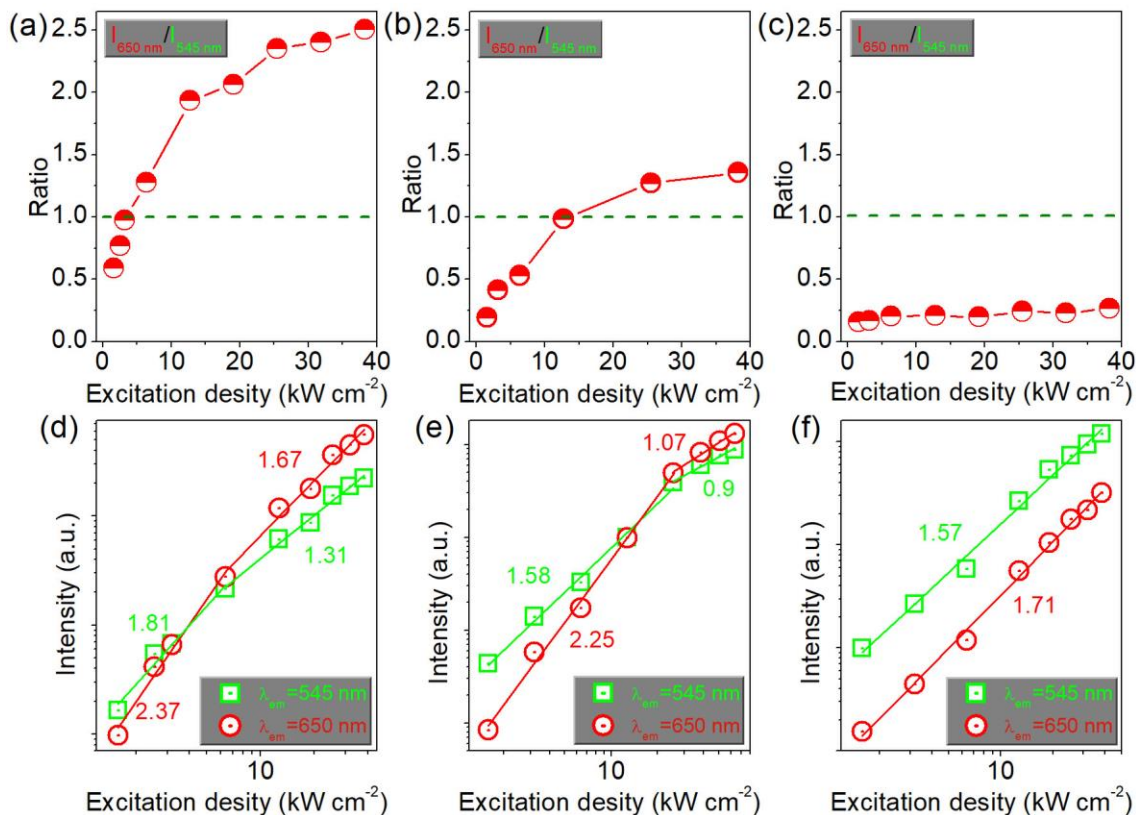


Fig. 3. The ratios of R/G for single (a) $\beta\text{-NaYF}_4:98\%\text{Yb},2\%\text{Er}$, (b) $\beta\text{-NaYF}_4:60\%\text{Yb},2\%\text{Er}$ and (c) $\beta\text{-NaYF}_4:20\%\text{Yb},2\%\text{Er}$ microcrystal as a function of the excitation intensity. The dependences of the UCL intensity on the excitation intensity for single (d) $\beta\text{-NaYF}_4:98\%\text{Yb},2\%\text{Er}$, (e) $\beta\text{-NaYF}_4:60\%\text{Yb},2\%\text{Er}$ and (f) $\beta\text{-NaYF}_4:20\%\text{Yb},2\%\text{Er}$ microcrystal. All excitation wavelengths are at ~ 808 nm.

To further investigate the UCL competition behaviors, we have calculated the ratios of red-to-green (R/G) UCL intensity for the single $\text{NaYF}_4:x\%\text{Yb},2\%\text{Er}$ microcrystal under different pump powers, as shown in Fig. 3a-c. For $\text{NaYF}_4:98\%\text{Yb},2\%\text{Er}$ microcrystal (Fig. 3a), the R/G ratios increase from 0.59 to 2.51 when the excitation intensity increases from 1.59 to 38.2 kW cm⁻². Moreover, the red and green UCL are

equivalent when the excitation intensity pumps at 3.18 kW cm^{-2} . However, Fig. 3b displays the R/G ratios rise merely from 0.19 to 1.36 as the excitation intensity gradually enhances. The excitation intensity for the red UCL exceeds the green one occurs at 12.7 kW cm^{-2} . Exceptionally, for $\text{NaYF}_4:20\% \text{Yb}, 2\% \text{Er}$ microcrystal shown in Fig. 3c, this R/G ratio keeps at ~ 0.20 which is independent to the excitation intensity. Fig. 3d-f shows the dependences of UCL intensity on the excitation intensity for $\text{NaYF}_4:x\% \text{Yb}, 2\% \text{Er}$ microcrystals doped with different Yb^{3+} concentrations. The slopes for the green and red UCL are all approximate to ~ 2 , which indicates that these two UCL are derived from the two-photon absorption processes. Notably, for doping with 98% and 60% Yb^{3+} concentrations of microcrystals, the red and green UCL appear saturation effects. In addition, the excitation intensity for the $\text{NaYF}_4:98\% \text{Yb}, 2\% \text{Er}$ microcrystal is lower than the $\text{NaYF}_4:60\% \text{Yb}, 2\% \text{Er}$ microcrystal. However, the UCL slope of $\text{NaYF}_4:20\% \text{Yb}, 2\% \text{Er}$ microcrystal is consistent under different excitation intensity due to without occurring of saturation effects.

Next, we further investigate the influence of doping Er^{3+} concentration on the UCL competition. Fig. 4a illustrates the ratios of R/G as a function of the excitation intensity for single $\beta\text{-NaYbF}_4:x\% \text{Er}$ microcrystals doped with different Er^{3+} concentrations. It reveals that the R/G ratios reduce as the doping Er^{3+} concentrations increase. Moreover, we make further efforts to explore the UCL properties for the single Er^{3+} -doped NaYF_4 microcrystal. Fig. 4b shows the UCL spectra of single $\beta\text{-NaYF}_4:2\% \text{Er}$ microcrystal under the excitation of 808 nm CW laser with different excitation density. The UCL spectra demonstrates that the green UCL is constantly larger than the red UCL and there is no UCL competition appearance. Therefore, its UCL color maintains green and is independent with the excitation intensity.

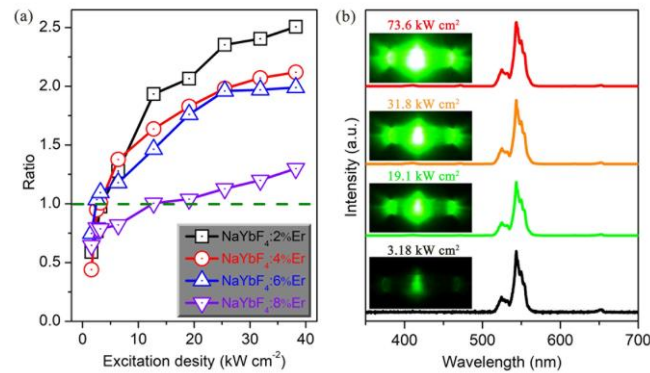


Fig. 4. (a) The ratios of R/G for single $\beta\text{-NaYbF}_4:x\% \text{Er}$ microcrystal doped with different Er^{3+} concentrations as a function of the excitation intensity. (b) The UCL spectra of single $\beta\text{-NaYbF}_4:2\% \text{Er}$ microcrystal under the excitation of 808 nm CW laser with different excitation density. The insert UCL photographs are corresponding to the relevant spectrum, respectively.

Having systematically demonstrated the experimental phenomenon, here we discuss the mechanism of the UCL competition induced by variation of excitation power. Fig. 5 gives the proposed UCL mechanism and possible routes for populating the upper emitting states of Er^{3+} ions. The corresponding UCL transitions as well as the energy-transfer (ET) processes are also provided. The population of the Er^{3+} ions can be divided in two steps: firstly, the electrons in the ground state of Er^{3+} are excited to the $^4\text{I}_{9/2}$ state by ground-state-absorption (GSA) or through ET from Yb^{3+} after absorbing the 808 nm photon; then continues to reach the $^2\text{H}_{9/2}$ state by absorbing a second 808 nm photon or $^4\text{I}_{11/2}$ state

through a non-radiative transition [25]. After that, the emitting states (${}^2\text{H}_{11/2}$, ${}^4\text{S}_{3/2}$, and ${}^4\text{F}_{9/2}$) can be populated by excited-state-absorption (ESA), CR, ET and non-radiative transition processes, which are clearly elaborated in Fig. 5. The significant population of the upper states of Er^{3+} ions can efficiently generate the UCL.

Notably, under the excitation of 808 nm laser, the doping Yb^{3+} concentrations will affect the populating routes for upper states of Er^{3+} . For highly Yb^{3+} -doped $\text{NaYF}_4:2\%\text{Er}$ microcrystal, the distance between the Yb^{3+} and Er^{3+} is relatively close, thus leads to the significant CR processes happening. The proposed CR processes are:

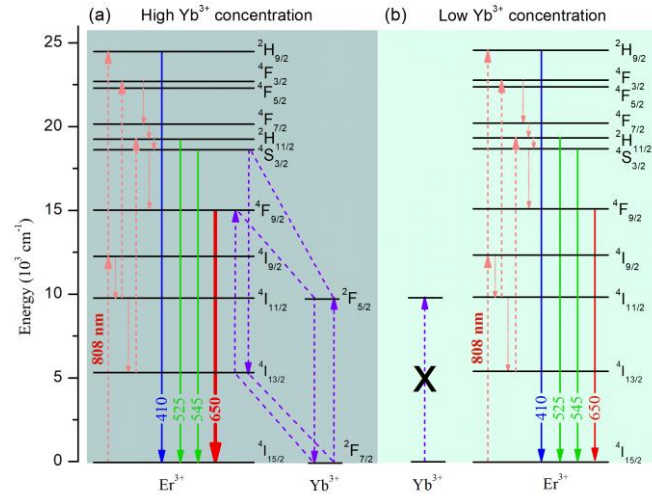
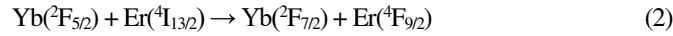
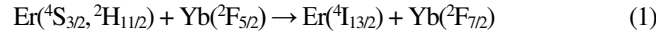


Fig. 5. The proposed energy level diagram for (a) highly Yb^{3+} -doped and (b) lowly Yb^{3+} -doped $\beta\text{-NaYF}_4:2\%\text{Er}$ microcrystals, the corresponding mechanism of ET processes, radiative and non-radiative transitions are also provided.

The above CR processes can efficiently enhance the population of red-emitting state (${}^4\text{F}_{9/2}$) and depopulate the green-emitting states (${}^4\text{S}_{3/2}$ and ${}^2\text{H}_{11/2}$). Therefore, under relatively lower excitation intensity, it mainly populates the green-emitting states, thus the green UCL is larger than red one and the UCL color tends to green. When gradually increase the excitation intensity, the CR processes become efficient, thus enhances the red UCL and suppresses green UC emissions. This causes the red and green UCL compete to each other. This experimental phenomenon is similar to our previous literature reported that the highly- Yb^{3+} doped $\text{NaYF}_4:\text{Er}$ microcrystals always tend to generate red UCL color under 980 nm excitation [23]. However, for lowly Yb^{3+} -doped $\text{NaYF}_4:2\%\text{Er}$ microcrystal, there is no CR processes occurrence because of the relatively far distance between Yb^{3+} and Er^{3+} ions. Therefore, the green- and red-emitting states maintain the same populating proportion as increases the excitation intensity, which results in the microcrystal keeping green UCL color.

4. Conclusions

In conclusion, we have systematically investigated the excitation power induced UCL competition in single $\text{NaYF}_4:x\%\text{Yb},2\%\text{Er}$ microcrystal under the excitation of 808 nm. It finds that, for highly Yb^{3+} -doped microcrystals, the red and green UCL compete to each other

and its UCL color can be finely tuned from green to orange when gradually increases the excitation intensity. On the contrary, there is no competition in lowly Yb³⁺-doped microcrystals and the UCL color retains green which is unchanged. The mechanism of the UCL competition is interpreted by CR processes owing to the short distance between Yb³⁺ and Er³⁺ ions in highly Yb³⁺-doped microcrystals. However, for lowly Yb³⁺-doped microcrystals, the long distance between Yb³⁺ and Er³⁺ ions prohibits the CR processes and the population of Er³⁺ ions keeps the original approaches, thereby creating the lowly Yb³⁺-doped NaYF₄:2%Er microcrystal facilitates green UCL color. Owing to the remarkable optical properties in micro-scale and particularly pumped at 808 nm laser, these microcrystals can be potentially applied in biological issues, aqueous environment and micro-optical devices.

Abbreviations

UCL: Upconversion luminescence; CW: Continuous-wave; CR: Cross-relaxation; SEM: Scanning electron microscopy; XRD: X-ray diffraction; R/G: Ratio of red-to-green; ET: Energy transfer; GSA: Ground-state-absorption; ESA: Excited-state-absorption.

Availability of Data and Materials

The datasets used and/or analysed during the current study are available from the corresponding author on reasonable request.

Competing Interests

The authors declare that they have no competing interests.

Funding

This work was financially supported by Natural Science Foundation of Guangdong Province (Grant No. 2016A030308010).

Authors' Contributions

MY and KH contributed the design of this research. MY, ZY and XY carried out the experiments. LW and RW contributed to the data analysis. SL provided the optical spectrum test and measurement. MY and ZY wrote the draft of manuscript. HW and XX revised and finalized the manuscript. All authors have read and approved the final manuscript.

Acknowledgments

Not applicable.

Author details

¹College of Advanced Interdisciplinary Studies, National University of Defense Technology, Changsha, 410073, China. ²State Key Laboratory of Pulsed Power Laser Technology, National University of Defense Technology, Changsha, 410073, China. ³Hunan Provincial Key Laboratory of High Energy Laser Technology, National University of Defense Technology, Changsha, 410073, China. ⁴Department of physics and

chemistry, PLA Army Academy of Special Operations, Guangzhou 510507, China. ⁵Guangdong Provincial Key Laboratory of Nanophotonic Functional Materials and Devices, School of Information and Optoelectronic Science and Engineering, South China Normal University, Guangzhou, 510006, China

References

1. Xu X, Li W, Hu C, Lei B, Zhang X, Li Y, Zhan Q, Liu Y, Zhuang J (2020) Promoting the growth of mung bean plants through uptake and light conversion of NaYF₄:Yb,Er@CDs nanocomposites. *ACS Sustain Chem Eng* 8:9751–9762
2. Liang L, Feng Z, Zhang Q, Cong TD, Wang Y, Qin X, Yi Z, Ang MJY, Zhou L, Feng H, Xing B, Gu M, Li X, Liu X (2021) Continuous -wave near-infrared stimulated-emission depletion microscopy using downshifting lanthanide nanoparticles. *Nat Nanotechnol* doi: 10.1038/s41565-021-00927-y
3. Liu H, Xu J, Wang H, Liu Y, Ruan Q, Wu Y, Liu X, Yang JKW (2019) Tunable resonator-upconverted emission (TRUE) color printing and applications in optical security. *Adv Mater* 31:1807900
4. Kaczmarek AM, Suta M, Rijckaert H, Van Swieten TP, Van Driessche I, Kaczmarek MK, Meijerink A (2021) High temperature (nano)thermometers based on LiLuF₄:Er³⁺, Yb³⁺ nano- and microcrystals. Confounded results for core-shell nanocrystals. *J Mater Chem C* 9:3589–3600
5. Zhou X, Smith BE, Roder PB, Pauzauskie PJ (2016) Laser refrigeration of ytterbium-doped sodium-yttrium-fluoride nanowires. *Adv Mater* 28:8658–8662
6. Rahman ATMA, Barker PF (2017) Laser refrigeration, alignment and rotation of levitated Yb³⁺:YLF nanocrystals. *Nat Photonics* 11:634–638
7. Liu Y, Teitelboim A, Fernandez-Bravo A, Yao K, Altoe M, Aloni S, Zhang C, Cohen BE, Schuck PJ, Chan EM (2020) Controlled assembly of upconverting nanoparticles for low-threshold microlasers and their imaging in scattering media. *ACS Nano* 14:1508–1519
8. Shang Y, Zhou J, Cai Y, Wang F, Fernandez-Bravo A, Yang C, Jiang L, Jin D (2020) Low threshold lasing emissions from a single upconversion nanocrystal. *Nat Commun* 11:6156
9. Wang Y, Zheng K, Song S, Fan D, Zhang H, Liu X (2018) Remote manipulation of upconversion luminescence. *Chem Soc Rev* 47:6473–6485
10. Wang F, Han Y, Lim CS, Lu Y, Wang J, Xu J, Chen H, Zhang C, Hong M, Liu X (2010) Simultaneous phase and size control of upconversion nanocrystals through lanthanide doping. *Nature* 463:1061–1065
11. Zhou J, Chen G, Wu E, Bi G, Wu B, Teng Y, Zhou S, Qiu J (2013) Ultrasensitive polarized up-conversion of Tm³⁺-Yb³⁺ doped β-NaYF₄ single nanorod. *Nano Lett* 13:2241–2246

12. Chen B, Liu Y, Xiao Y, Chen X, Li Y, Li M, Qiao X, Fan X, Wang F (2016) Amplifying excitation-power sensitivity of photon upconversion in a NaYbF₄:Ho nanostructure for direct visualization of electromagnetic hotspots. *J Phys Chem Lett* 7:4916
13. Hossain MY, Hor A, Luu Q, Smith SJ, May PS, Berry MT (2017) Explaining the nanoscale effect in the upconversion dynamics of β -NaYF₄:Yb³⁺, Er³⁺ core and core-shell nanocrystals. *J Phys Chem C* 121:16592–16606
14. Wen S, Zhou J, Schuck PJ, Suh YD, Schmidt TW, Jin D (2019) Future and challenges for hybrid upconversion nanosystems. *Nat Photonics* 13:828–838
15. Zhang Y, Yu Z, Li J, Ao Y, Xue J, Zeng Z, Yang X, Tan TTY (2017) Ultrasmall-superbright neodymium-upconversion nanoparticles via energy migration manipulation and lattice modification: 808 nm-activated drug release. *ACS Nano* 11:2846–2857
16. Liu B, Li C, Yang P, Hou Z, Lin J (2017) 808-nm-light-excited lanthanide-doped nanoparticles: rational design, luminescence control and theranostic applications. *Adv Mater* 29:1605434
17. Huang X (2015) Giant enhancement of upconversion emission in (NaYF₄:Nd³⁺/Yb³⁺/Ho³⁺)/(NaYF₄:Nd³⁺/Yb³⁺) core/shell nanoparticles excited at 808 nm. *Opt Lett* 40:3599–3602
18. Li C, Zhang C, Hou Z, Wang L, Quan Z, Lian H, Lin J (2009) β -NaYF₄ and β -NaYF₄:Eu³⁺ microstructures: morphology control and tunable luminescence properties. *J Phys Chem C* 113:2332–2339
19. Wang T, Yu H, Siu CK, Qiu J, Xu X, Yu SF (2017) White-light whispering-gallery-mode lasing from lanthanide-doped upconversion NaYF₄ hexagonal microrods. *ACS Photonics* 4:1539–1543
20. Chen B, Kong W, Liu Y, Lu Y, Li M, Qiao X, Fan X, Wang F (2017) Crystalline hollow microrods for site-selective enhancement of nonlinear photoluminescence. *Angew Chem Int Edit* 56:10383–10387
21. Chen B, Sun T, Qiao X, Fan X, Wang F (2015) Directional light emission in a single NaYF₄ microcrystal via photon upconversion. *Adv Opt Mater* 3:1577–1581
22. Han Q, Gao W, Zhang C, Mi X, Zhao X, Zhang Z, Dong J, Zheng H (2018) Tunable flower-like upconversion emission and directional red radiation in a single NaYF₄:Yb³⁺/Tm³⁺ microcrystal particle. *J Alloy Compd* 748:252–257
23. Yuan M, Wang R, Zhang C, Yang Z, Cui W, Yang X, Xiao N, Wang H, Xu X (2018) Exploiting the silent upconversion emissions from a single β -NaYF₄:Yb/Er microcrystal via saturated excitation. *J Mater Chem C* 6:10226–10232
24. Gao D, Wang D, Zhang X, Feng X, Xin H, Yun S, Tian D (2018) Spatial control of upconversion emission in a single fluoride microcrystal via the excitation mode and native interference effect. *J Mater Chem C* 6:622–629
25. Yang X, Wang L, Wang R, Yang Z, Song C, Yuan M, Han K, Lan S, Wang H, Xu X (2021) Achieving tunable multicolor display and sensitive temperature sensing in self-sensitization of erbium-doped CaF₂ nanocrystals under 808, 980 and 1532 nm irradiation. *Opt Mater Express* 11:2514–2527